ISSN: 2447-3359

REVISTA DE GEOCIÊNCIAS DO NORDESTE

Northeast Geosciences Journal

v. 10, nº 1 (2024)

https://doi.org/10.21680/2447-3359.2024v10n1ID31682

Electrical resistivity tomography and seismic refraction in slope assessment: the case of Mirante Slope, Guarujá-São Paulo

Tomografia de resistividade elétrica e sísmica de refração na avaliação de encostas: o caso da Encosta do Mirante, Guarujá-São Paulo

Cleber de Jesus Santos[1]; Jefferson de Lima Picanço[2]; Otávio Coaracy Brasil Gandolfo[3]; Marcelo César Stangari[4]; Julia Vieira Santo[5]; Luca Lämmle[6]

[1] Department of Geology and Natural Resources, Institute of Geosciences, University of Campinas (UNICAMP), Campinas, Brazil. Email: c264746@dac.unicamp.br
ORCID: https://orcid.org/0000-0001-5450-2004

[2] Department of Geology and Natural Resources, Institute of Geosciences, University of Campinas (UNICAMP), Campinas, Brazil. Email: jeffepi@unicamp.br
ORCID: https://orcid.org/0000-0003-1631-1818

[3] Cities, Infrastructure and Environment Department, Institute for Technological Research (IPT) São Paulo, Brazil. Email: gandolfo@ipt.br
ORCID: https://orcid.org/0000-0003-2883-0463

[4] Institute of Astronomy, Geophysics and Atmospheric Sciences, University of São Paulo (USP), São Paulo, Brazil. Email: cesar.stangari@iag.usp.br
ORCID: https://orcid.org/0009-0005-6020-6048

[5] Department of Geology and Natural Resources, Institute of Geosciences, University of Campinas (UNICAMP), Campinas, Brazil. Email: j238364@dac.unicamp.br
ORCID: https://orcid.org/0009-0001-9947-1245

[6] Department of Geography, Institute of Geosciences, University of Campinas (UNICAMP), Campinas, Brazil. Email: lucalammle@ige.unicamp.br
ORCID: https://orcid.org/0000-0001-6668-3914

Abstract: The occurrence of landslides in mountainous regions due to rainfall has been motivating intense discussions about the search for mechanisms to monitor hydrological processes at a detailed scale. Geophysics emerges as an alternative methodology in overcoming this challenge, given its practicality in obtaining data, spatial resolution, and cost/benefit ratio, besides using non-invasive methods. Thus, the objective of this research is to explore the potential of the combined use of the Refraction Seismic method with Electrical Resistivity Tomography in the evaluation of slopes associated to landslides, especially from different climatic contexts. For this purpose, the regolith was characterized using both methods. Additionally, the slope was monitored in two different climatological scenarios, dry and rainy periods. In this opportunity, the aspects related to the correlations between the tomography information to understand the water-regolith dynamics will also be presented. The combination of methods made it possible to identify the hydrological conditions of the investigated subsurface in a comprehensive way, either at the top, in the slipped material, or at the base of the slope. The combination of the geoelectric method, capable of mapping the saturation in the soil, combined with the refraction seismic method, capable of identifying horizons with different mechanical properties, allowing for a more secure and detailed interpretation of the subsurface, for example, structures associated with soil movement, as well as low resistivity anomalies in the form of pockets, possibly related to the leakage in the transmission network of the water treatment plant. In addition, the methodological strategy allowed the identification at the base of the slope of the influence of the salt wedge. Considering the benefits of the combination of both methods, it is believed that the increase of geophysical information in geotechnical monitoring can contribute decisively to improve the understanding of slope instability mechanisms.

Keywords: Electrical Resistivity Tomography; Seismic Refraction; Landslides; Serra do Mar.

Resumo: A ocorrência de escorregamentos em regiões serranas devido as chuvas vêm motivando intensas discussões acerca da busca por mecanismos de monitoramento dos processos hidrológicos em escala de detalhe. A geofísica desponta como uma metodologia alternativa na superação deste desafio, dada a sua praticidade na obtenção dos dados, resolução espacial, relação custo/benefício, para além de utilizarem métodos não invasivos. Assim, o objetivo da pesquisa consiste em explorar as potencialidades do uso combinado do método de Sísmica de Refração com a Tomografia de Resistividade Elétrica na avaliação de encostas associadas a escorregamentos, sobretudo a partir de contextos climáticos distintos. Para tal, foi realizada uma caracterização do regolito através de ambos os métodos. Adicionalmente executou-se um monitoramento da encosta em dois cenários climatológicos distintos, período seco e chuvoso. Na oportunidade, serão apresentados também os aspectos relativos às correlações entre as informações das tomografias para compreender a dinâmica da água-regolito. A combinação de métodos possibilitou identificar as condições hidrológicas da subsuperfície investigada de forma abrangente, seja no topo, no material escorregado e na base da encosta. A combinação do método geoelétrico, capaz de mapear a saturação no solo, aliado ao método sísmico de refração, capaz de identificar horizontes com propriedades mecânicas diferentes, permitiu uma interpretação mais segura e detalhada do subsolo, a exemplo de estruturas associadas a movimentação do solo, bem como anomalias de baixa resistividade na forma de bolsões, possivelmente relacionadas ao vazamento na rede de transmissão da estação de tratamento de água. Além disso a estratégia metodológica permitiu identificar na base da encosta a influência da cunha salina. Considerando o constatado benefício proveniente da combinação de ambos os métodos apresentados, acredita-se que o incremento de informações de geofísica no monitoramento geotécnico, pode colaborar de forma decisiva melhoria na compreensão dos mecanismos de instabilização de encosta.

Palavras-chave: Tomografia de Resistividade Elétrica; Sísmica de Refração; Deslizamentos de Terra; Serra do Mar.

Received: 02/03/2023; Accepted: 04/09/2023; Published: 15/03/2024.

1. Introduction

Geophysical studies applied to slope characterization have been developed using various methodologies (BOGOSLOVSKY et al., 1977; PALMER; WEISGARBER, 1988; MCCANN; FORSTER, 1990; GÖKTÜRKLER et al., 2008; IMANI, 2021; SANTOS et al., 2021; LÄMMLE et al., 2022a; LÄMMLE et al., 2022b). Detailed investigations through the combination of geophysical methods are within this context and are of significant relevance for a better understanding of landslide initiation (CRAWFORD; BRYSON, 2018). The geotechnical challenge in evaluating landslide-prone areas is associated with both geological complexities, due to the movement and mixing of layers, and operational limitations in depth of investigation and access to the entire area due to rugged terrain. Therefore, geotechnical inspections have been relying on geophysical methods to overcome these challenges, given the proven ability to image extensive areas continuously and with satisfactory lateral and depth resolution in a practical manner. To address limitations and complement geotechnical analysis, indirect methods have been increasingly employed, such as geophysics (ISMAIL; TAIB; ABAS, 2019; PICANÇO et al., 2019), which proves to be an effective methodology in these cases due to its ability to investigate regolith with accurate and precise spatial-temporal resolution.

Geophysical methods enable the investigation of extensive areas through continuous measurements in the regolith, both laterally and in depth. Being a non-destructive methodology, geophysics does not require numerous drillings and sample collections (BURGER; SHEEHAN; JONES, 2006). The evolution of instruments and acquisition techniques has allowed for the collection of significant volumes of data with satisfactory precision, as well as continuous improvement in computational capacity, resulting in increasingly advanced mathematical processing, high-resolution imaging, and detailed assessments (JONGMANS and GARAMBOIS, 2007). However, the geophysical approach has limitations related to potential ambiguities in result interpretation, hindering the precise characterization of the geological environment. This can be resolved through the appropriate combination of techniques and/or the use of direct methods such as borehole drilling, geological mapping, among others.

The Refraction Seismic Method involves the investigation of the subsurface by analyzing refracted waves in geological layers. Wave velocity is sensitive to variations in physical properties of the medium, such as density and elastic parameters (Poisson's ratio, bulk and shear moduli, etc.). This allows for the estimation of sediment composition, porosity, water saturation, as well as geotechnical parameters such as shear strength (KEAREY, 2002; KAMINSKY, 2013). On the other hand, Electrical Resistivity Tomography (ERT) is based on the distribution of electrical resistivity in subsurface geological materials. It can accurately identify water content, saturation, structures, and lithotypes without the need for direct sampling and recognition (LEHMANN et al., 2013; BRAGA, 2016).

It is understood that the combined use of geophysical methods enhances the ability to interpret images, improving the ability to distinguish geological structures that cannot be visualized with a single methodology (HACK, 2000). The proposal to combine the refraction method and ERT aims to improve accuracy and safety in diagnostics, as well as to address possible ambiguities commonly encountered in areas affected by landslides due to geological heterogeneity (BARTA et al., 2005). In this context, discussions based on the combination of methods, semi-automated acquisitions, and the use of modern geophysical data processing techniques have grown significantly and have contributed to the advancement of the field. However, literature on the integrated use of geophysical methods in slope assessment in Brazil is still in its early stages.

The study involves the joint use of Refraction Seismics and Electrical Resistivity Tomography on slopes associated with landslides in the municipality of Guarujá/SP. Two acquisition campaigns were conducted (dry and rainy seasons), with 4 electrical profiling lines at 3m and 5m spacings obtained in each campaign, as well as a third campaign for the acquisition of 4 seismic refraction lines with 10m spacing between geophones. An integrated analysis of the techniques was then established to facilitate discussions regarding the identification and differentiation of geological materials within the regolith and the monitoring of saturation domain distributions. It is understood that, despite the significant number of research studies on the topic, few have sought to provide evidence through the integration of geophysical methods.

2. Materials and Methods

2.1 Study Area

The study area is located on the forested escarpment of an isolated hill in the vicinity of the Marinas do Guarujá condominium, in the Cidade Jardim Tom neighborhood, Guarujá-SP (UTM coordinates 276691.157E and 7353271.514N DATUM– SIRGAS2000/Zone 23K), a region known for its tourism activities in the Baixada Santista (Figure 1).

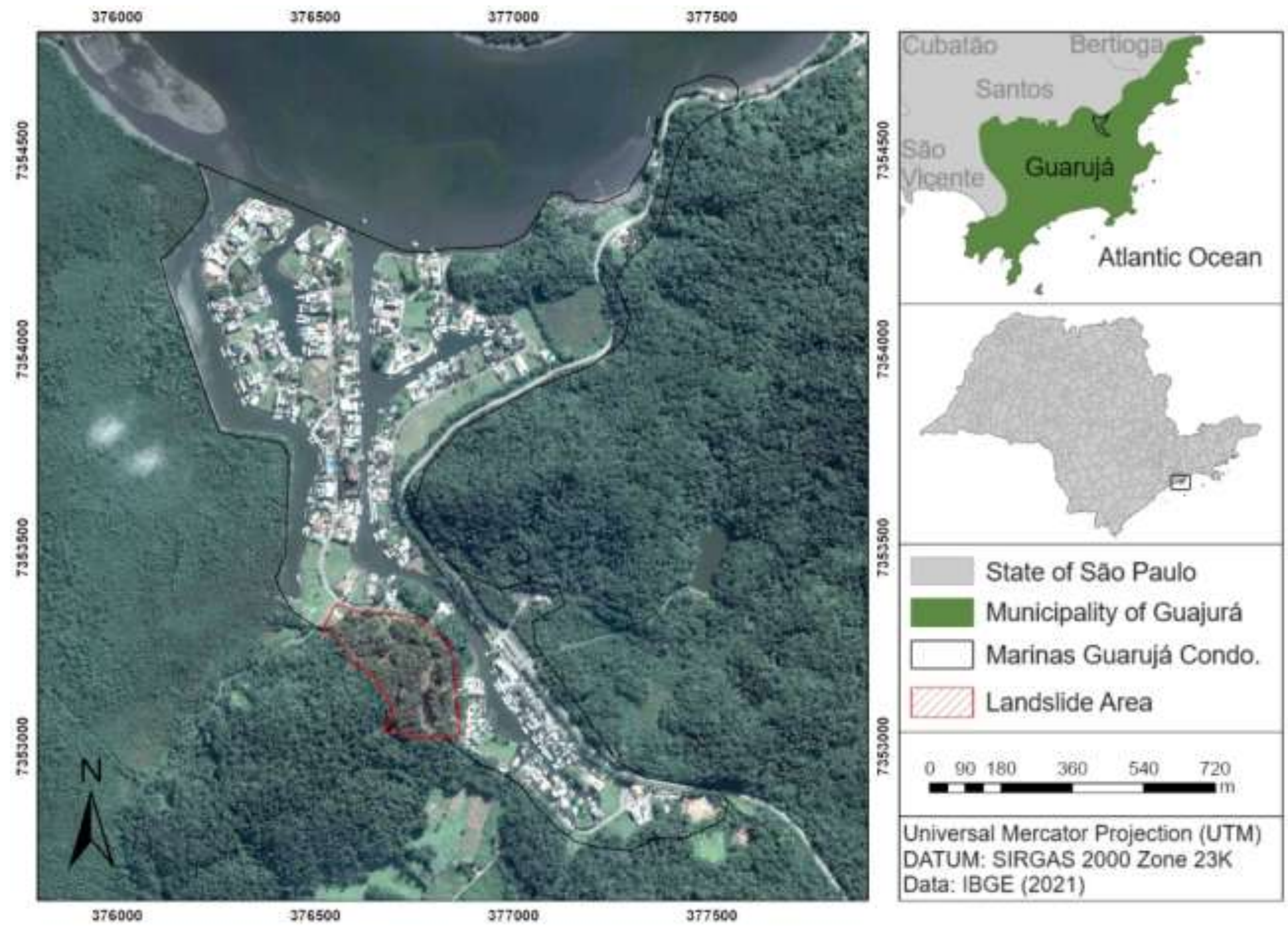

Figure 1 – Location of the study area.
Source: Own authorship.

The topography of the Guarujá municipality is predominantly composed of flat areas, along with isolated hills with a maximum altitude of 320m and an average slope of around 30% (CORSI; MACEDO, 2016). The hillside areas have witnessed intense urban development in recent decades, leading to deforestation and erosional processes, contributing to landslides (CORSI; MACEDO, 2016). The geological context of the Guarujá municipality includes the presence of gneisses, granites, and metasediments from the Ribeira Belt (TUPINAMBÁ, 2012). The substrate of the study area consists of paragneisses, peraluminous gneisses, biotite gneiss, and calc-silicate rocks (IPT, 2020). Generally, these mentioned lithotypes are covered by thick regolith with finer grain sizes, predominantly clayey, and more micaceous (Figure 2).

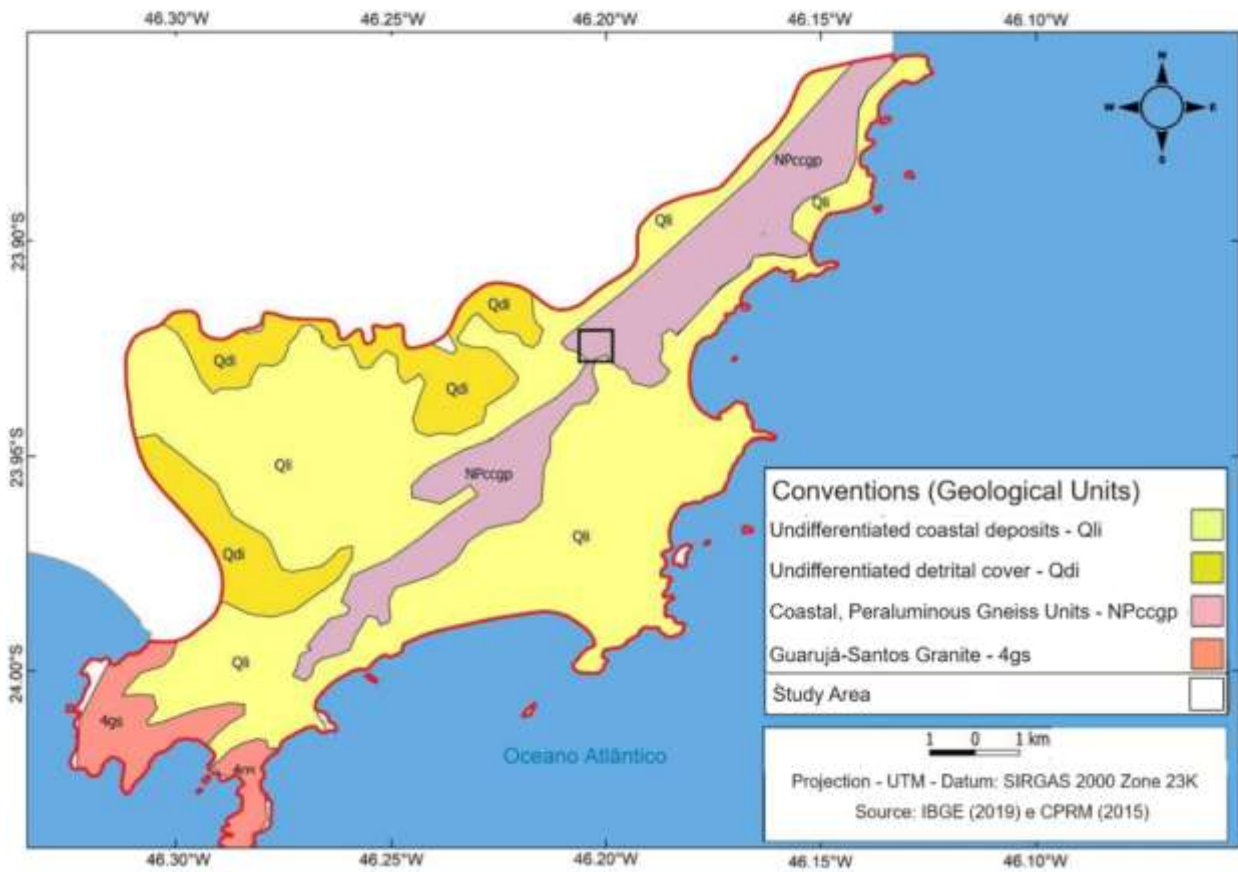

Figure 2 – Main geological units in the municipality of Guarujá-SP.
Source: Own authorship.

2.2 Seismics refraction

Refraction is the phenomenon associated with the change in direction and velocity of a wave when it passes from a less dense medium to a denser one. Thus, refraction seismic is the method of investigating the physical properties of the geological medium by measuring, processing, and interpreting the arrival time of the refracted seismic wave in the subsurface (CARDARELLI, 2002). In the conducted work, refraction seismics were used to complement electrical resistivity tomography data. While the electrical resistivity method can identify the distribution of water with good sensitivity, seismic refraction, using S-wave, map the distribution of velocity in the solid matrix of the geological layers because the S-wave is relatively insensitive to the presence of water.

Consider a model with two geological layers (1 and 2) containing a source emitting S-waves and a receiver as shown in figure 3a below. For refraction to occur, the seismic wave velocity in layer 2 must be greater than the velocity in layer 1 (Figure 3a). Refraction seismics use the transit times of the first arrivals at the receivers positioned at a certain critical distance (Xcritical) from the energy source. This can be observed in figure 3b, which relates the offset distance (source-receiver) to the wave travel time, where after Xcritical (Figure 3b), the refracted wave overtakes the direct wave traveling at the velocity of medium V_1.

In the context of a two-layer model with horizontal interfaces, Snell's Law can be expressed as $\sin\theta = \frac{v_1}{v_2}$ or $\cos\theta = \sqrt{\left(1 - \frac{v_1^2}{v_2^2}\right)}$, and the total travel time (t) of a critically refracted seismic wave in a lower layer along the path ABCD (Figure 3a) is given by:

$$t = \frac{x}{v_2} + \frac{2z\cos(\theta_c)}{v_1} \quad [1]$$

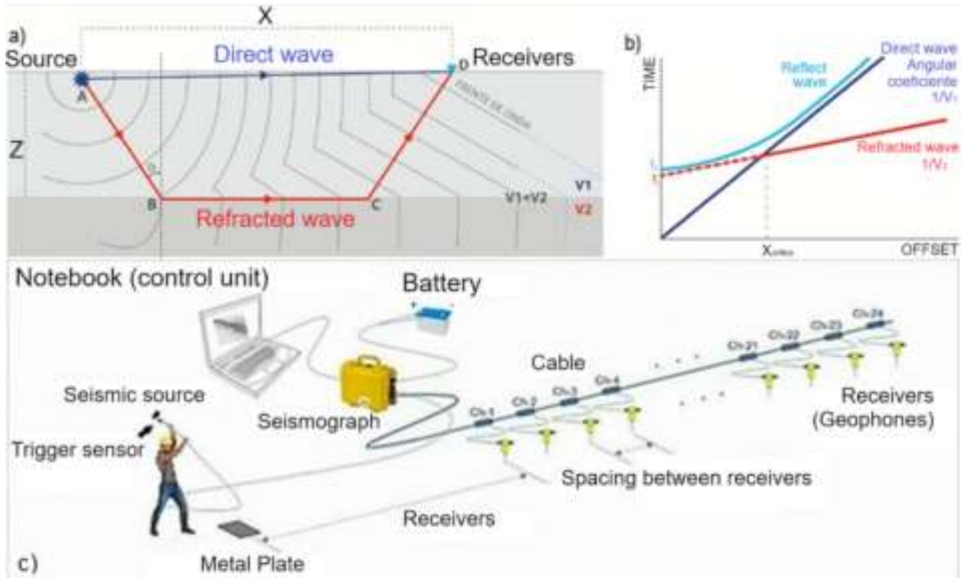

Figure 3 – a) Representative diagram of the refraction seismic phenomenon considering a two-layer model. b) Relationship between the seismic wave travel time and the distance from the source to the receiver. c) Representative diagram of the refraction seismic survey.
Source: Adapted from HGI (2023).

In figure 3c, we have a schematic representation of the basic equipment used in the field for collecting refraction seismic data. The technique employs a 5kg sledgehammer connected to a trigger sensor that generates a seismic wave source. Twenty-four horizontal-component geophones with a natural frequency of 28Hz were spaced at 4m intervals, along with an offset of the same distance, forming a seismic spread of 100m to record the arrival time of the refracted wave. The signal was recorded on a Geode seismograph (Geometrics) with 24 channels in the form of seismic shots, meaning the recording of arrival times at the 24 receivers. Finally, the data underwent preprocessing with the application of gains and filters (in the frequency domain, velocity inversion). For the processing step, SeisImager SW software was used for noise removal and inversion, resulting in a velocity model with depth.

Figure 4 – a) Geophysical data survey (a) Line 1; (b) Line 2; (c) Line 3.
Source: Own authorship.

In planning the data acquisition, the following operational aspects were taken into account: i) define the area of interest; ii) consider the required investigation depth, with the method's capability estimated at approximately 1/5 of the length of the investigation line; iii) estimate the appropriate number of channels to ensure good horizontal resolution (CARDARELLI, 2002). The field arrangement used in collecting refraction seismic data consisted of positioning the shot offsets along a line parallel to the geophones. Meanwhile, the source was positioned at approximately half the interval distance between the geophones (Figure 3c).

2.3 Electrical Resistivity Tomography (ERT)

The electrical resistivity method is a geophysical investigation technique that relies on mapping the distribution of electrical resistivity (ρ) in the subsurface. This type of investigation occurs by injecting a continuous electric current or very low-frequency current through two electrodes (A and B), followed by measuring the potential difference (ΔV) between two regularly spaced electrodes (M and N) (Figure 3). The physical principles of the method are based on the theories of electricity and electromagnetism (KIRSCH; YARAMANCI, 2006; LOKE, 2016). According to Ward (1990), for a point source injecting a current of intensity I into the interior of a homogeneous and isotropic conductive half-space with resistivity, representing a flat Earth, the electric potential at an observation point P, located at a distance r from the source electrode, is given by:

$$V(r) = \frac{I\rho}{2\pi r} \quad [2]$$

As the potential function is a scalar quantity, the total potential from various sources can be obtained by adding the contributions from each source separately. Applying this principle to the quadrupole, the potential difference between points M and N, generated by the injection of currents at points A and B, is given by:

$$\Delta V = \frac{I\rho}{2\pi}\left(\frac{1}{AM} - \frac{1}{BM} - \frac{1}{AN} + \frac{1}{BN}\right) \quad [3]$$

Where,

$$k = 2\pi\left(\frac{1}{AM} - \frac{1}{BM} - \frac{1}{AN} + \frac{1}{BN}\right)^{-1} \quad [4]$$

or,

$$\rho = k\frac{\Delta V}{I} \quad [5]$$

In which k is referred to as the geometric factor of the array, as it depends solely on the relative arrangement of the electrodes in the field. The equation is used to calculate the resistivity of a homogeneous and isotropic medium. However, in practice, due to the heterogeneous nature of the rock, the subsurface cannot be considered a homogeneous medium. Therefore, the reading taken by the equipment represents resistivity considering a homogeneous medium, which is why the resulting resistivity is termed apparent. This parameter represents the outcome of measurements from some of the geoelectric methods (BRAGA, 2006). For heterogeneous and/or anisotropic media, the resistivity calculated in this way varies with the position and/or orientation of the electrode array (GANDOLFO, 2007).

In the data acquisition, an experimental arrangement is also established according to the established objectives. The data collection procedure was carried out using the Dipole-Dipole array. The choice of this type of array is due to the possibility of taking readings both laterally and in depth, which is a practical and dynamic option for data collection (BRAGA, 2016; GANDOLFO, 2007), in addition to being one of the methods that best identifies lateral variations in resistivity. In the Dipole-Dipole array, the investigation occurs along lines in a fixed direction, where the current electrodes (AB) and potential electrodes (MN) have a constant spacing (Figure 4). Each distance (R) between the centers of electrode pairs (AB and MN) corresponds to a depth of investigation. Finally, measurements are taken by increasing the distance (R) proportionally in the direction of the traverse to scan the resistivity and induced polarization of the soil (Figure 4).

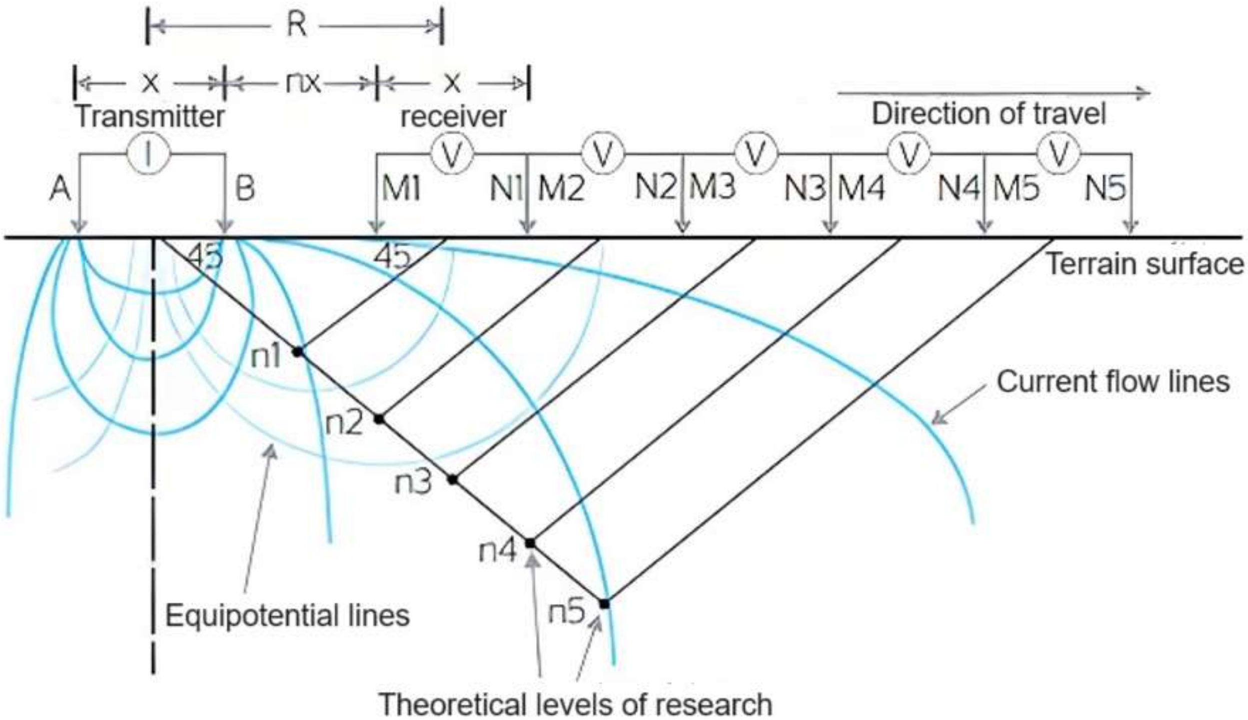

Figure 4 – a) Schematic illustrating the dipole-dipole arrangement used in the field.
Source: Own authorship.

Tomography involves automated electrical profiling that yields a considerably larger number of measurements than conventional profiling. The execution of this type of profiling requires high-tech equipment that enables automated measurements. Due to the processing of a large volume of data, tomography provides images with a high spatial resolution (CHAMBERS et al. 2014; WHITELEY, 2019). The application of Electrical Resistivity Tomography in the context of geotechnical issues, such as landslides, aims to identify hydrogeological aspects of subsurface materials by producing a two-dimensional electrical image. Through this, we can obtain information about saturation, fractures or voids, and hydraulic conductivity.

Electrical resistivity (ER) data were collected using the Rho/IP system, consisting of a Syscal R2 resistivity meter acting as a receiver, with 10 channels, operating in conjunction with a current transmitter connected to a 250 W DC/DC converter and a 12 V battery. The data were acquired using the semi-automatic electrical profiling technique with the dipole-dipole array in two different configurations, one with a 5m and another with a 3m spacing between electrodes. The equipment has a control panel that allows for data preview in the field and adjustments to the device's configuration. The hardware includes internal data storage and an input for transferring acquired field data. The resistivity data processing was performed using the Res2Dinv software, which consisted of preprocessing, inversion, and 2D modeling steps.

Figure 5 – a) Rho/IP system used in the electrical path, 1(receiver), 2(transmitter), 3(DC/DC converter), 4(battery). b) Data survey on Line 4.
Source: Own authorship.

2.4. Sampling and experimental design

The methodological procedures were organized into 3 stages. The first stage was dedicated to the preliminary area reconnaissance, defining the spatial scope of the study, and setting the data collection points. The second stage involved field data acquisition, which was further divided into two phases: seismic survey and geoelectric survey. The third stage was dedicated to data processing and interpretation.

To assess the subsurface geological materials, electrical profiling lines and refraction seismic lines were executed along monitoring lines positioned for the study (Figure 6). Measurements were conducted during the late dry season in September 2022. The sampling grid established for the research consists of 4 lines [Lines 1 (L1); Line 2 (L2); Line 3 (L3); Line 4 (L4)], located at the top of the slope (L1 and L2), in the landslide material (L3), and at the base of the slope (L4) (Figure 6). The quantity and distribution of the established lines were based on the slope's geometry, adhering to regular sampling criteria, ensuring the adequate investigation of the slope's top, colluvial materials, and the base of the slope.

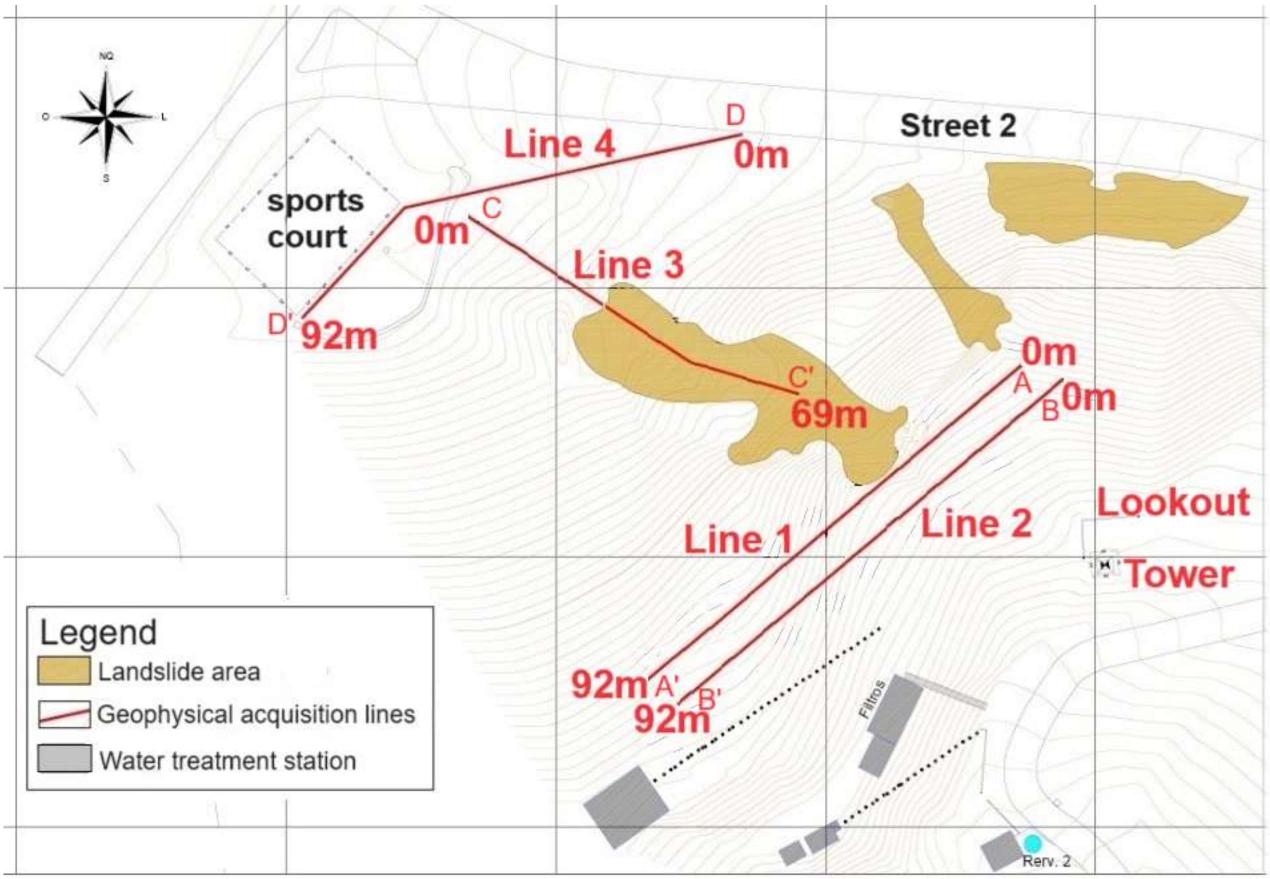

Figure 6 – Location of the lines of interest for the acquisition of refraction seismic and electrical resistivity tomography data.
Source: Own authorship.

In the first stage, four technical visits were made with the assistance of the civil defense team of the municipality of Guarujá to assess the dimensions of landslide areas, open paths, and preliminary geological mapping in the area. During this time, we also marked the geophysical survey lines. The second stage began with the refraction seismic survey along the four lines (Figure 6) in the first half of 2021.

In each line, acquisition was conducted using two different spacings (5 and 3 meters). The tomography obtained from the electrical profiling with 5m spacing reached greater depths, while the profiling with 3m spacing provided more detailed information about subsurface bodies. Additionally, the use of both spacings in the electrical profiling allowed for a comparative analysis of both images, enhancing the level of interpretation and avoiding potential ambiguities.

The first campaign was conducted at the end of the dry climatic period (September) to establish a baseline for monitoring moisture distribution over time and space. The second campaign was carried out at the beginning of the rainy climatic period (December).

The geophysical data were qualitatively interpreted by comparing the results with reference values established in the literature for each geological material. Furthermore, the interpretation was based on the comparative analysis of both geophysical methods to assess data consistency and eliminate potential ambiguities. Finally, all the information collected in the research was compared to the information obtained from geological mapping and available literature.

3. Results and Discussions

3.1. Seismic refraction

The refraction seismic investigation was conducted along the four pre-established lines (L1, L2, L3, and L4) for the preliminary recognition of the weathering profile. In general, it was possible to identify a model with three layers with distinct velocities. The velocities suggest a relatively thin, organic-rich surface soil layer. Just below that, there is an excavable residual soil layer, followed by a more consolidated soil layer. The maximum depth reached with refraction seismic varied between 10 and 12 meters in the lines positioned at the top of the slope and in the landslide material, L1, L2, and L3, respectively. Furthermore, it was not possible to identify the top of the intact rock in the refraction seismic sections (Figure 7).

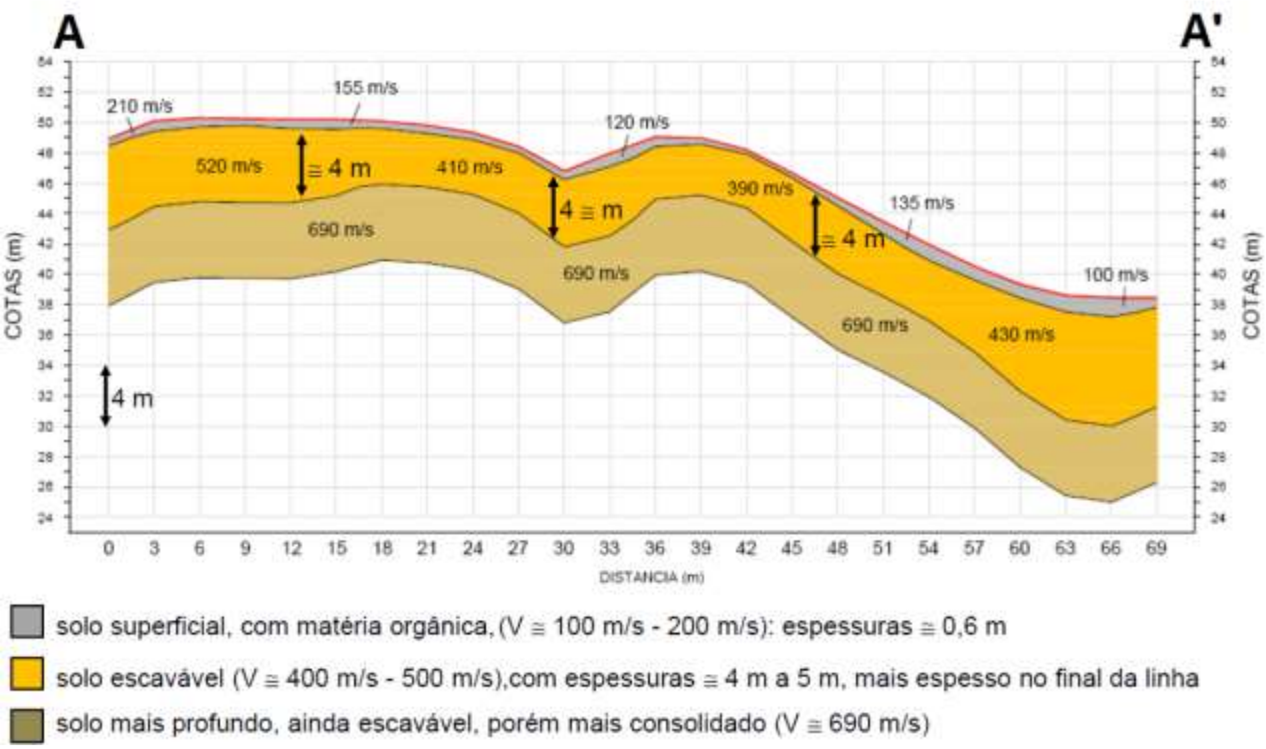

Figure 7 – Refraction seismic results carried out on Line 1 (L1), top of the slope.
Source: Own authorship.

The refraction seismic survey conducted on line 2 generated a velocity model that follows the same pattern as line 1, with three layers. A shallow layer with low velocity, between 150 and 250 m/s (gray), is followed by a thicker intermediate layer, between 420 and 550 m/s (yellow), suggesting a poorly consolidated sandy-silt material (excavable). Finally, a third layer, between 720 and 780 m/s (brown), represents the same geological material with a higher degree of consolidation, being impenetrable by manual auger drilling. The seismic interface that limits the intermediate layer coincided with the maximum depth (~5.95m) reached in manual auger drilling, conducted near stake 16 (E16). This maximum excavable depth is associated with the geotechnical boundary (Figure 8).

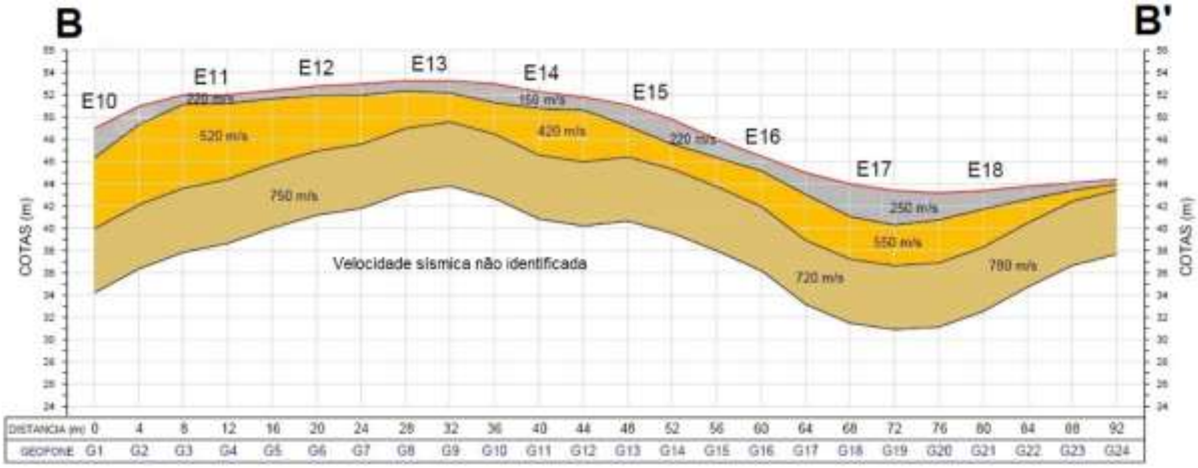

Figure 8 – Seismic model for Line 2. Source: Own authorship.
Source: Own authorship.

Among the investigated lines (L1, L2, L3, L4), line 3 (L3) stands out, as its velocity model showed discrepant values. The model obtained for line L3 contains two layers, with the first layer (gray) having velocities between 130 - 230 m/s, a velocity pattern that suggests a disaggregated and highly porous geological material in the shallow layer context. In the intermediate layer (yellow), velocities vary laterally between 400 m/s and 800 m/s, and the third layer could not be identified with refraction seismic. The considerable lateral variation corresponds to the relatively porous and permeable nature of the geological material commonly identified in colluvial deposits, especially in the upper layers of the line of interest (Figure 9).

It is understood that the movement process undergone during deposition causes the landslide material to have a heterogeneous pattern in grain size distribution, inclined layers, and the possibility of buried organic matter. This non-uniform distribution of geological materials results in a non-homogeneous pattern in seismic velocity distribution. As in lines 1 and 2, the seismic velocity model presented in line 3 does not indicate the presence of intact rock at the investigated depth.

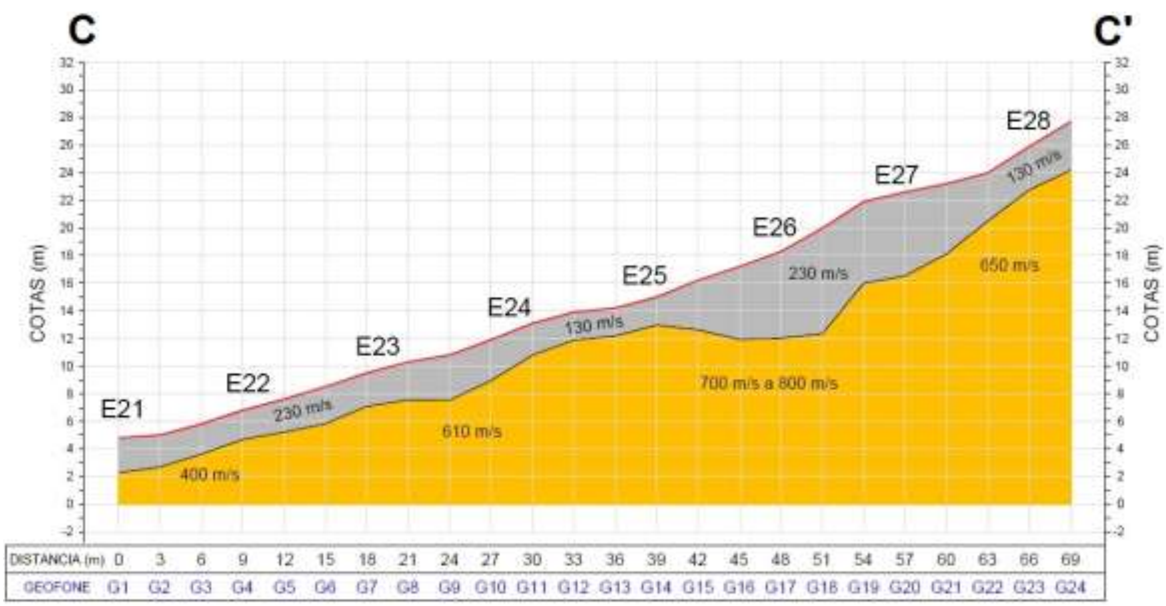

Figure 9 – Inferred seismic model for line 3, on the hillside.
Source: Own authorship.

Line 4 is positioned outside the slope and adjacent to the condominium road. The reason for positioning this line is related to the need for a record with minimal influence from the landslide. The seismic section on line 4 presents a model of three layers with distinct velocities, with the first layer having velocities between 160 and 430 m/s, suggesting a base soil used for road construction (in the first 20m of the line) and a geological fill material (from 20m onwards), both possibly associated with the urbanization works of the Marinas Guarujá condominium. The second seismic layer shows a velocity of 740 m/s across its entire length, indicating a continuous and homogeneous residual soil layer at first. Just below, the model identified velocities greater than 2000 m/s, a characteristic context of altered rock. It is worth noting that, although not delimited, it was in the deepest sector of line 4 where the velocity pattern came closest to the intact rock (Figure 10).

Figure 10 – Inferred seismic model for line 4.
Source: Own authorship.

3.2. Electrical Resistivity Tomography (ERT)

3.2.1. Top of the slope

The geoelectric model in figure 12 presents the result of electrical profiling along Line 1 followed by Line 2, both located at the top of the slope with a 7m spacing. The maximum depth reached in the sections was approximately 15m. The shallow zone (up to 0,6m) in both geoelectric sections (Figure 11) showed slight divergences, possibly associated with local variations in the amount of organic matter, the presence of water, or even local variations in lithological components, a fact that can be observed to some extent in other geoelectric sections.

Overall, it is possible to identify two main domains in sections 1 and 2. The left domain shows predominantly high resistivities (>3000 Ω.m) compared to the right domain. In the left domain, high resistivity anomalies occur in circular shapes, which may suggest the presence of highly altered rock, hitherto unidentified in the refraction seismic data (Figure 11).

In the section of lines 1 and 2, between 65 and 80m, there is a low resistivity anomaly (<300 Ω.m), indicating saturation conditions up to a depth of 7.5m in both sections. In the deeper domains, we notice a trend towards standardization, with more laterally uniform resistivity values, which is more evident in Line 1. At the maximum investigated depth, it was not possible to identify the water table (Figure 11). Here, you can observe the influence of the topography on the signal, where lower areas accumulate thicker sedimentary layers and have more humid soils. This saturated domain may be related to suspended aquifers originating from impermeable layers like rock fragments or due to the irregular distribution of wet areas in the regolith, or even areas of clay concretions, which is less likely given the type of terrain and pedology.

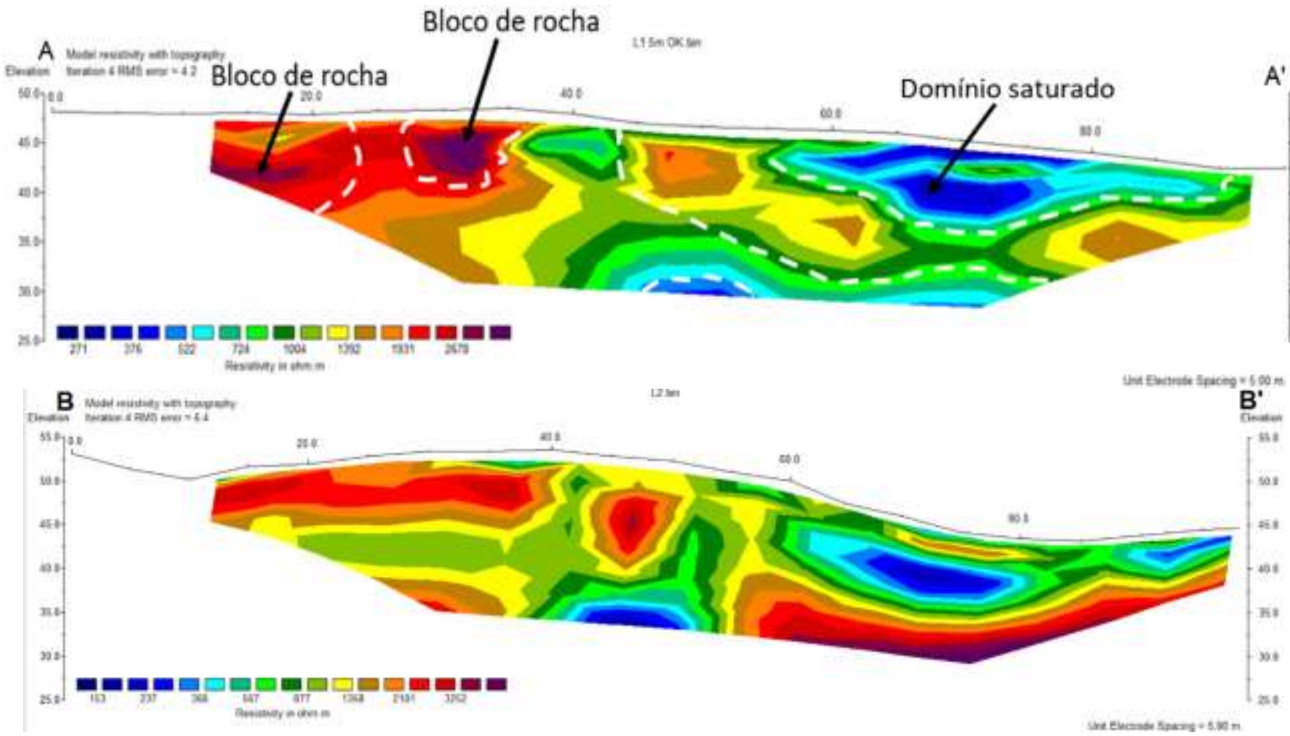

Figure 11 – Electrical resistivity tomography (ERT) of lines 1 and 2, approximately 7m apart laterally and located at the top of the slope.
Source: Own authorship.

In the joint analysis of refraction seismic and electrical resistivity tomography data, the data show a satisfactory correspondence between the methods. The geotechnical boundary identified in the field with manual auger at stake 15 of Line 2 coincided with the resistivity values in the tomography of this line. The velocity values in the 3rd layer (brown) (Figure 8) are consistent with the resistivity values between 12 and 15m depth in Line 2, B-B' Figure (11), along almost the entire length.

3.2.2. Slumped material

The idea of conducting electrical profiling along the slope aimed to provide details about the geological materials within the first 10 meters of depth, assess the distribution of moisture in depth, its variations over time (dry and rainy seasons), detect preferential domains of infiltrated water percolation, and identify the presence of bedrock.

Due to operational considerations such as the relationship between the array size and the limited length of the line, the decision was made not to perform electrical profiling with a 5-meter electrode spacing. Therefore, the electrical profiling was conducted only with a 3-meter electrode spacing. In this context, the resistivity model was able to image the subsurface to a maximum depth of approximately 10 meters but couldn't identify the static water level.

The profile exhibited considerable variations in resistivity values, which are associated with the natural complexity of the landslide material. The large textural variability, the presence of rock fragments, and soil movement due to gravity-driven transport account for the significant variability in the data.

The profile shows a vertically oriented anomaly of low resistivity in the center of the section. This anomaly is consistent with the rainy climatic conditions. The presence of a drainage system crossing the section perpendicular to the line may be related to this anomaly.

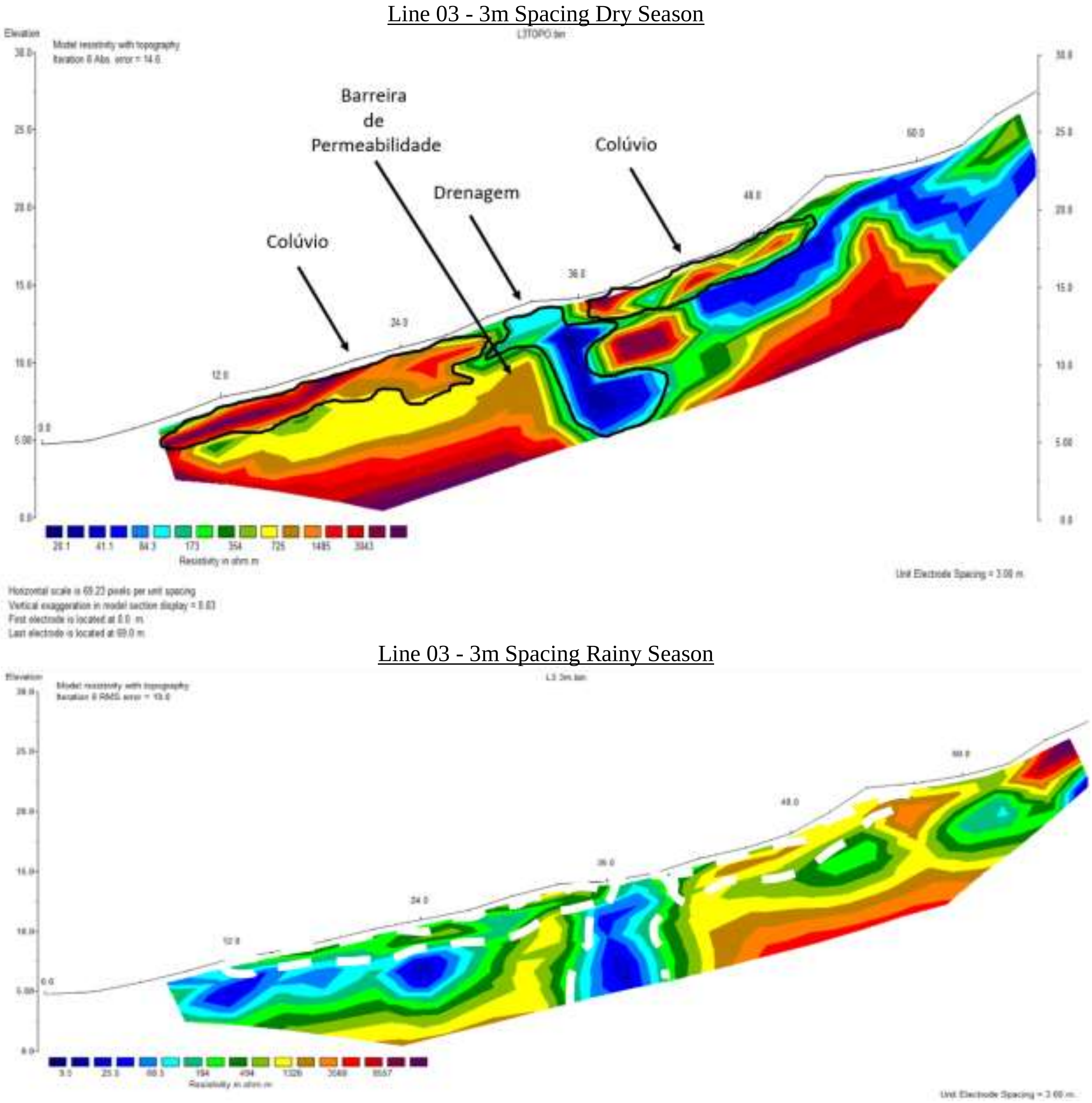

Figure 12 – Electrical Resistivity Tomography (ERT) L3, located on the slope in different climatic periods (dry and rainy).
Source: Own authorship.

In the analysis of ERT data during both dry and rainy periods, in conjunction with refraction data, it becomes evident that regardless of the rainfall variation between readings, there are two distinct domains delimited by a vertically oriented anomaly of low resistivity. The first domain extends from the beginning of the line to the 36-meter mark, followed by a second domain upslope from 36 meters. In the second domain, the landslide material exhibits significant heterogeneity in resistivity values and considerable variations in resistivity from the dry to rainy periods, indicating a highly porous and permeable material. In contrast, the first domain displays a more homogeneous resistivity pattern with little variation in resistivity values between dry and rainy periods, suggesting lower permeability and greater consolidation compared to the second domain.

3.2.3. Base of Slope

The electrical resistivity survey corresponding to line 4 was conducted at the base of the slope and adjacent to the condominium road. Similar to the refraction survey, the results exhibited a resistivity pattern with layers showing lateral continuity, in contrast to the other sections. This suggests that line 4 was minimally affected by the recent landslide that occurred on Morro do Mirante.

The resistivity model was obtained from the electrical survey conducted with both 5 and 3 meters of electrode spacing. In both sections of L4, resistivity values above 700 Ω.m were identified in the first 5 meters of depth, particularly in the first 50 meters of the line. This feature is well pronounced in the section and may suggest modified soil for road construction (Figure 13).

During the transition to the rainy season, a slight reduction in resistivity patterns was observed, indicating the influence of moisture on subsurface resistivity distribution, although the resistivity pattern persisted. From a depth of 5 meters, resistivity values decreased considerably (<200), with most values being below 100 Ω.m, both at the end of the dry season and during the transition to the rainy season. The change in resistivity values in relation to the shallower layers is influenced by both groundwater from the slope in the first 40 meters of the line and the saline wedge in the last 60 meters.

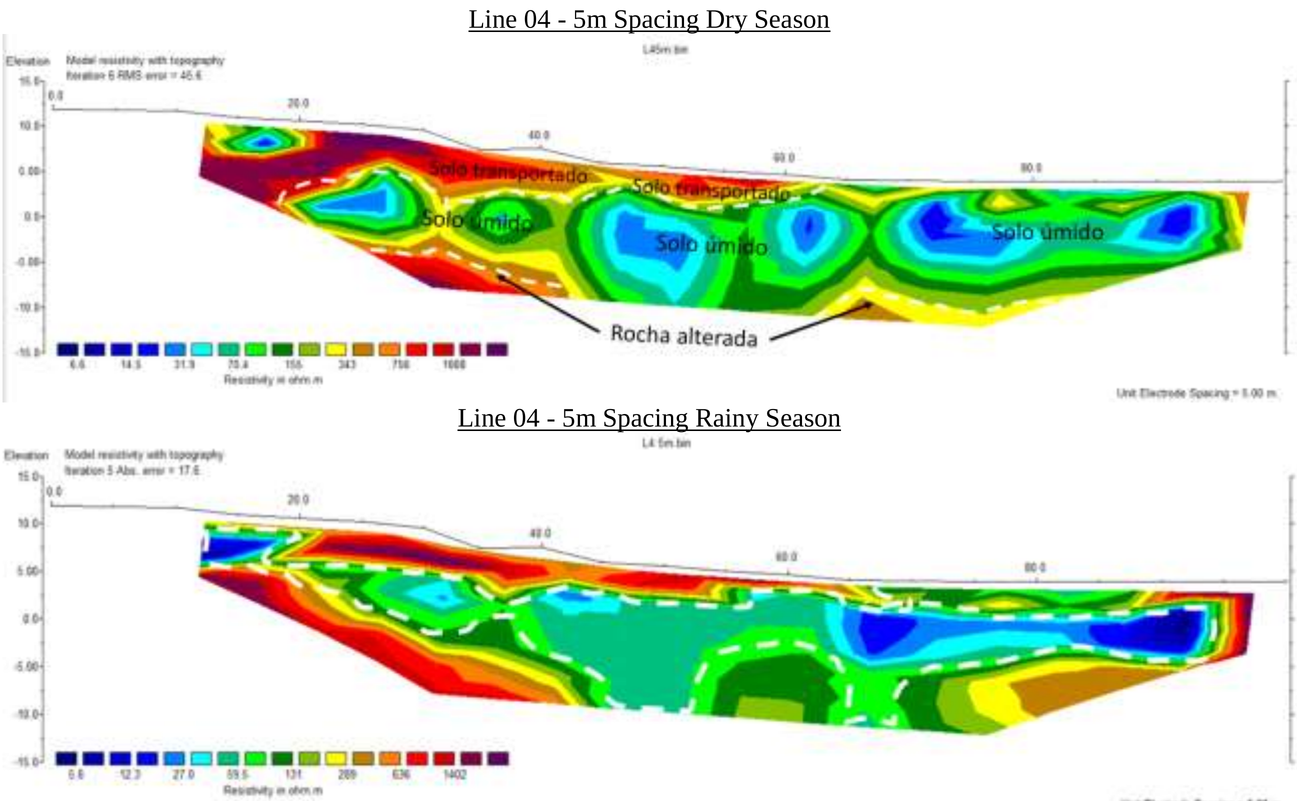

Figure 13 – Geo-electric section L4 with 5m spacing, located on the slope in different climatic periods (dry and rainy). Source: Own authorship.

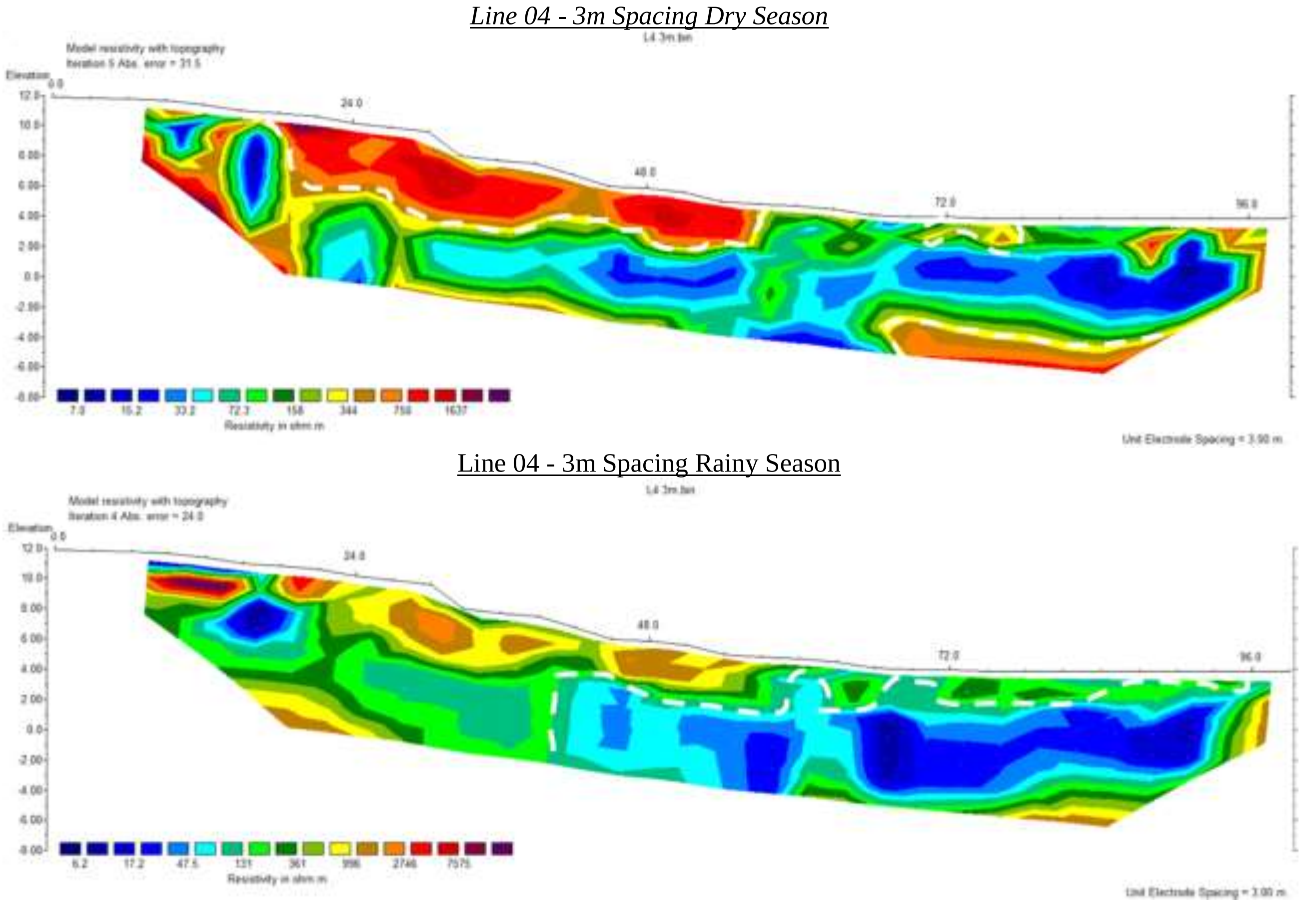

Figure 14 – Electrical Resistivity Tomography (ERT) L4 with 3m spacing, at the base of the slope in different climatic periods (dry and rainy).
Source: Own authorship.

Analyzing line 4 (Figures 10, 13, and 14) using both methodologies (refraction and ERT), we can identify geology that has been less affected by the landslide compared to what was observed in other lines. The lateral continuity of seismic and geoelectric strata corresponds satisfactorily, implying the same geological setting: a superficial layer in the form of transported soil followed by a more cohesive soil in contact with altered rock. The predominance of features with electrical resistivity aligns with the location of line 4, as it represents an area of groundwater discharge. In the moisture models, it was also possible to infer the static water level at the base of the slope.

We can see from the analysis of the figures above the contributions resulting from the integration of the aforementioned techniques (IMANI et al., 2021). For example, while refraction reached greater depths, electrical resistivity tomography provided better resolution, especially for delineating water bodies, due to its sensitivity to the presence of water. Additionally, refraction does not allow for velocity inversion of layers in depth, a limitation overcome by ERT.

The results allowed for a more precise identification and characterization of the different regolith levels of the Mirante Slope and the distribution of moisture in different hydrological contexts. The ability to image the soil laterally through electrical surveying offers a broader and more continuous view of the slope compared to conventional methods, identifying variations in resistivity and their relationship with lithological and hydrological aspects. Operational limitations, such as difficult access due to dense vegetation and the steep slope of the slope, sometimes hindered a more extensive geophysical mapping.

The methodological framework used demonstrated significant efficiency in geotechnical analysis of slope regolith. The proposal to use modern computational techniques for data processing and the strategy of simultaneously acquiring a large volume of data enabled improved characterization and recognition of geological materials at depth. Furthermore, the combination of certain geophysical methodologies with direct characterization approaches is a promising tool to complement conventional geotechnical studies in slope areas.

Considering the geological, geomorphological, geotechnical, and geophysical aspects developed so far, it is believed that the area requires further conclusive studies regarding the degree of terrain stability and consequently the risk of future mass movements. Although it is not an area of high population density, it is worth noting the extreme environmental fragility of the study area. The silty-clayey, extremely moist nature of the soils present (as observed in both dry and rainy seasons) favors a loss of cohesion, which, combined with unfavorable geomorphological conditions, represents a danger to the population, especially when exposed to intense rainfall episodes.

4. Final Considerations

The results obtained in this study demonstrate that the methodological approach used represents a powerful assessment tool for slope areas, providing an accurate view of the regolith in the landslide-affected area and thus offering a basis for safer and more effective geotechnical inspections. However, this does not negate the need for analysis through direct methods, such as in-situ measurements and laboratory analysis of soil samples.

The combination of seismic and electrical methods has confirmed their complementary nature, considering the issue of landslides, enabling a broader and more secure geotechnical diagnosis compared to conventional methods. The correspondence between the results (ERT and SR) demonstrates the high quality of the acquired data. The investigation carried out in the landslide material identified significant variations in physical properties, both in the seismic and geoelectric models, highlighting the potential of the methodological approach in characterizing geological materials in landslide-prone slopes. Nevertheless, this does not rule out the need for additional analysis through direct methods.

Overall, the soil exhibits a pattern with low resistivity values, suggesting a moist area, even during dry periods. This is associated with the climatic context of the region with a high rainfall index, as well as the characteristics of the present soil. In general, the silty-clayey soil has a high hydraulic hysteresis. This characteristic allows water to infiltrate relatively easily into the surface during rain, while, during the dry period, some of this water ends up being retained in narrower pores, resulting in slower water drainage.

Tomography monitoring, carried out in two different climatic periods (dry and rainy), allowed for the qualitative distinction of significant changes in resistivity values. Through this technique, it was possible to infer variations in moisture and hydraulic conductivity, delineate rock blocks, and identify the extent of movement at depth.

The study area has young residual soil, of silty-clayey nature, with a notable presence of extremely altered gneissic rock fragments. At the top of the slope, the minimum depth of intact rock can be identified at some points at approximately 8m, with the superficial layers exhibiting a more silty and less compacted behavior. At greater depths, this soil tends to be more clayey and compacted. In this compartment of the slope, the soil exhibited indicative patterns of differential movement in the transverse direction, suggesting local slope variations at points of the same elevation. It is also worth noting that in this compartment of the slope, specifically at the end of lines 1 and 2, the low resistivity anomalies remained consistent in both dry and rainy periods, indicating a continuous process of water infiltration into the slope. This context is possibly associated with the presence of the water treatment station adjacent to lines 1 and 2.

Along the landslide material, the presence of bedrock occurs at some points, between 6 and 7.5m in depth, with significant lateral variations in geophysical data, clearly associated with differential movement at various depth levels. The integrated ERT analysis between the dry and rainy periods in the landslide material revealed a hydrological context consisting of a verticalized low-resistivity anomaly separating two domains of the landslide material at the 36m mark of line 3. While in the first half of the line, we have a more homogeneous resistivity pattern, in the second half, we have a more heterogeneous pattern. It is worth noting that in the comparative analysis (dry and rainy periods), two geological materials with different degrees of consolidation and permeability are observed. This suggests the presence of two materials corresponding to landslides that occurred at different times, with the material above related to the 2020 landslide, while the geological material located below the permeability barrier corresponds to a previous landslide.

Due to the environmental fragility presented in the study area, it is opportune to conduct geotechnical intervention studies in the domains of the studied area to make the construction of new residential establishments viable.

Detailed investigation of hydrological aspects in landslide-prone slopes is an emerging topic that has been providing significant contributions to the improvement of conventional geotechnical investigations. Therefore, investing in the continuity of research of this nature is timely, aimed at better understanding this complex and challenging phenomenon.

Acknowledgments

The authors would like to thank the State University of Campinas - Unicamp for the institutional support, the National Council for Scientific and Technological Development - CNPq through the CNPq/MCTI/FNDCT Call No. 18/2021 - universal range a - 405565/2021-6, led by researcher Ana Elisa Abreu, and the Coordination for the Improvement of Higher Education Personnel - CAPES for the financial support. We also appreciate the cooperation of the Institute of Technological Research - IPT and the University of São Paulo - USP for providing the necessary infrastructure for the development of the geophysical work.

References

BÁRTA, J., DOSTÁL, D.; BENEŠ, V.; TESAR, M. Application of Geophysical Methods in The Study of Landslide Movements, Taking Into Account Geological Conditions in The Study Mountains, *Acta Geodynamica et Geomaterialia*, 2, 121-129. 2005.

BBC, British Broadcasting Corporation. 2023. *Dozens die as deadly storm hit Brazilian coast*, Online. Disponível em: https://www.bbc.com/pidgin/articles/cpwj29d231po, Data de acesso: 21/02/2023.

BOGOSLOVSKY, V. A.; OGILVY, A. A. Geophysical methods for the investigation of landslides. *Geophysics*, vol. 42, no. 3, pp. 562–571, 1977.

BRAGA, A. C. O. *Geofísica Aplicada: métodos geoelétrico em hidrologia*. São Paulo: Oficina de Textos, 2016.

BRAGA, A. C. O. *Métodos da Eletrorresistividade e Polarização Induzida Aplicados nos Estudos da Captação e Contaminação de Águas Subterrâneas*: uma Abordagem Metodológica e Prática, Tese (livre docência), Universidade Estadual Paulista, Rio Claro-SP, Brasil, 2006.

BURGER, H. R.; SHEEHAN, A. F.; JONES, C. H. *Introduction to Applied Geophysics:* Exploring the Shallow Subsurface. [s.l.] W.W. Norton, 2006.

CARDARELLI, E. Ray tracing in elliptical anisotropic media using the linear traveltime interpolation (LTI) method applied to traveltime seismic tomography. *Geophysical Prospecting*, v. 50, n. 1, p. 55-72, 2002.

CASTRO, J. M. G. *Pluviosidade e movimentos de massa nas encostas de Ouro Preto*. Dissertação (Mestrado em Ciências da Engenharia Civil). Universidade Federal de Ouro Preto, Ouro Preto, 138 p, 2006.

CHAMBERS, J. E.; GUNN, D. A.; WILKINSON, P. B.; et al. 4D electrical resistivity tomography monitoring of soil moisture dynamics in an operational railway embankment. *Near Surface Geophysics*, v. 12, n. 1, p. 61–72, 2014.

CORSI, A. C.; MACEDO, E. S. de. *Plano Municipal de Redução de Risco do Município de Guarujá*. 16o Congresso Brasileiro de Geologia de Engenharia e Ambiental. Anais. 2016.

CRAWFORD, M. M.; BRYSON, L. S. *Assessment of active landslides using field electrical measurements*. Engineering Geology, v. 233, n. June 2017, p. 146–159, 2018b.

DE BARI, C.; LAPENNA, V.; PERRONE, A.; et al. Digital photogrammetric analysis and electrical resistivity tomography for investigating the Picerno landslide (Basilicata region, southern Italy). *Geomorphology*, v. 133, n. 1–2, p. 34–46, 2011.

GANDOLFO, O. C. B. *Um estudo do imageamento geoelétrico na investigação rasa*. 2007. Tese (Doutorado em Recursos Minerais e Hidrogeologia) - Instituto de Geociências, Universidade de São Paulo, São Paulo, 2007. Acesso em: 2022-12-19.

GÖKTÜRKLER, G.; BALKAYA, Ç.; ERHAN, Z. Geophysical Investigation of A Landslide: The Altındağ landslide site, İzmir (western Turkey). *Journal of Applied Geophysics*, v. 65, n. 2, p. 84–96, 2008.

HACK, R. Geophysics for slope stability. *Surveys in Geophysics*, v. 21, n. 4, p. 423–448, 2000.

HGI, HydroGeophysics - Geophysical Consulting. Seismic Aq Example Graphic. hgiworld.com, 2023. Disponível em: < https://www.hgiworld.com/methods/seismics/seismic-multi-channel-analysis-of-surface-waves-masw/seismic-aq-example-graphic-hydrogeophysics/>. Acesso em: 08/03/2023.

IMANI, P.; EL-RAOUF, A. A.; TIAN, G. Landslide investigation using Seismic Refraction Tomography method: a review. *Annals of Geophysics*, v. 64, n. 6, p. 27, 26 jan. 2021.

IPT - Instituto de Pesquisas Tecnológicas do Estado de São Paulo. *Estudos Técnicos para a criação de Unidade de Conservação (UC) na Serra de Santo Amaro, Guarujá-SP*. São Paulo. Relatório Técnico-Parcial n º 159 752-205. 2020.

IPT. Instituto de Pesquisas Tecnológicas. *Relatório Técnico no 93: Plano Municipal de Redução de Risco do Município do Guarujá*. São Paulo: IPT, 2007.

ISMAIL, N. EL H.; TAIB, S.; ABAS, F. Slope monitoring: an application of time-lapse electrical resistivity imaging method in Bukit Antarabangsa, Kuala Lumpur. *Environmental Earth Sciences*, v. 78, 2019.

JABOYEDOFF, M.; OPPIKOFER, T.; ABELLAN, A.; et al. Use of LIDAR in landslide investigations: A review. *Natural Hazards*, v. 61, n. 1, p. 5–28, 2012.

JONGMANS, D.; GARAMBOIS, S. Geophysical investigation of landslides: A review. *Bulletin de la Societe Geologique de France*, v. 178, n. 2, p. 101–112, 2007.

KEAREY, P.; BROOKS, M., HILL, I., *An Introduction to Geophysical Exploration. Blackwell*, London. p. 262, 2002.

KIRSCH, R.; YARAMANCI, U. *Geophysical characterisation of aquifers*, Groundwater Geophysics, Springer, Germany, 2006.

LÄMMLE, L.; PEREZ FILHO, A.; DONADIO, C.; ARIENZO, M.; FERRARA, L.; SANTOS, C. J.; SOUZA, A. O. Anthropogenic Pressure on Hydrographic Basin and Coastal Erosion in the Delta of Paraíba do Sul River, Southeast Brazil. *Journal of Marine Science and Engineering*, v. 10, p. 1585, 2022b.

LÄMMLE, L.; PEREZ FILHO, A.; DONADIO, C.; MOREIRA, V. B.; SANTOS, C. J.; SOUZA, A. O. Baixos terraços marinhos associados às transgressões e regressões marinhas holocênicas na Planície Costeira do rio Paraíba do Sul, Rio de Janeiro, Brasil. *Revista Brasileira de Geomorfologia*, v. 23, p. 1285-1303, 2022a.

LEHMANN, P.; GAMBAZZI, F.; SUSKI, B.; et al. Evolution of soil wetting patterns preceding a hydrologically induced landslide inferred from electrical resistivity survey and point measurements of volumetric water content and pore water pressure. *Water Resources Research*, v. 49, n. 12, p. 7992–8004, 2013.

MCCANN, D. M.; FORSTER, A. *Reconnaissance geophysical methods in landslide investigations*. Engineering Geology, v. 29, n. 1, p. 59–78, 1990.

MCKEAN, J.; BUECHEL, S.; GAYDOS, L. *Remote-Sensing and Landslide Hazard Assessment*. Photogrammetric Engineering and Remote Sensing, v. 57, n. 9, p. 1185–1193, 1991.

METTERNICHT, G.; HURNI, L.; GOGU, R. *Remote sensing of landslides: An analysis of the potential contribution to geo-spatial systems for hazard assessment in mountainous environments*. Remote Sensing of Environment, v. 98, n. 2–3, p. 284–303, 2005.

PALMER, D. F.; WEISGARBER, S. L. *Geophysical Survey of the Stumpy Basin Landslide*, Ohio, Environment Engineering Geoscience, xxv, p. 363-370, 1988.

PAULO, M. S. M. F.; ADAN, R. P. *Movimentações de massa ocorridas em Guarujá/SP no mês de março de 2020*. Trabalho de Conclusão de Curso (Graduação - Engenharia Ambiental) Instituto do Mar, Universidade Federal de São Paulo, 2021. Santos, p. 63, 2021.

PETLEY, D. Global patterns of loss of life from landslides. *Geology*, v. 40, n. 10, p. 927–930, 2012.

PICANÇO, J. L.; MESQUITA, M. J.; MELO, L. L. Geotechnical and Mineralogical Properties of Granite Regolith Related to Nucleation Mechanisms of Debris Flows in Tropical Areas. *International Journal of Erosion Control Engineering*, v. 11, p. 54-62, 2019.

ROSIN, P. L.; HERVÁS, J. Remote sensing image thresholding methods for determining landslide activity. *International Journal of Remote Sensing*, v. 26, n. 6, p. 1075–1092, 2005.

SANTOS, C. J.; LÄMMLE, L.; MOREIRA, V. B.; PICANÇO, J. L.; MINCATO, R. L.; AYER, J. E. B. Avaliação da qualidade da água em aquífero raso em Campos dos Goytacazes, Rio de Janeiro, Brasil. *Revista Brasileira de Geografia Física*, v. 14, p. 3241-3254, 2021.

SOLANKI, A.; GUPTA, V.; BHAKUNI, S.S.; et al. Geological and geotechnical characterisation of the Khotila landslide in the Dharchula region, NE Kumaun Himalaya. *Journal of Earth System Science*, v. 128, n. 4, p. 86, 22 jun. 2019.

TUPINAMBÁ, M.; TEIXEIRA, W.; HEILBRON, M. *Evolução tectônica e magmática da Faixa Ribeira entre o Neoproterozoico e o Paleozoico Inferior na região serrana do Estado do Rio de Janeiro, Brasil*. Anuário do Instituto de geociências–UFRJ, v. 35, n. 2, p. 140-150, 2012.

WARD, S. *Resistivity and Induced Polarization Methods*, Geotechnical and Environmental Geophysics, Vol. 1, SEG, 147-189, 1990.

WARD, W. O. C.; WILKINSON, P.; CHAMBERS, J.; et al. Distribution based fuzzy clustering of electrical resistivity tomography images for interface detection. *Geophysical Journal International*. v. 197, p. 310–321, 2014.

WHITELEY, J. S. et al. Geophysical Monitoring of Moisture-Induced Landslides: A Review. *Reviews of Geophysics*, v. 57, n. 1, p. 106–145, 2019.